

Observation of High-Energy Electrons Accelerated by Electrostatic Waves Propagating Obliquely to a Magnetic Field

Yasushi Nishida and Naoyuki Sato

Department of Electrical Engineering, Utsunomiya University, Utsunomiya, Tochigi 321, Japan
(Received 9 March 1987)

It is revealed in microwave-plasma interaction experiments that a large-amplitude electrostatic wave propagating obliquely to a magnetic field accelerates electrons strongly *almost* along the magnetic field lines via the process of $V_p \times B$ acceleration. The experimental results are in reasonable agreement with the theoretical prediction of Sugihara *et al.*

PACS numbers: 52.75.Di, 52.40.Nk, 52.50.Gj

When an electrostatic wave (ω, k) (the electron plasma wave, for example) propagates in the z direction, *perpendicularly* ($\theta = \pi/2$, θ the angle between k and B) to a magnetic field B (x direction), an electron trapped in the wave trough is accelerated in the direction $(-e)V_p \times B = A_y$ (y direction), where $V_p = \omega/k$ is the phase velocity of the electrostatic wave. The process has been theoretically studied by Sagdeev and Shapiro¹ and Sugihara and Midzuno.² Dawson *et al.*³ investigated this acceleration when the wave electric field E was so strong that the trapping velocity $(eE/mk)^{1/2}$ was comparable to the phase velocity. Nishida and co-workers^{4,5} have experimentally proved the existence of this acceleration process and reasonably good agreement with the theoretical predictions is obtained. Therefore, this mechanism (abbreviated as $V_p \times B$ acceleration) is characterized by the fact that a dc field appearing in the wave frame accelerates a trapped particle.

In the present Letter we would like to show the first experimental observation in which the electrostatic wave (ES wave) with a trapped particle in its trough propagates in the z direction, *obliquely* ($\theta \neq \pi/2$) to the magnetic field which should appear as $B = B_x = B_0 \sin \theta$ in the $V_p \times B$ acceleration mechanism [see Fig. 1(b)]. As the magnetic field has the component $B_z = B_0 \cos \theta$, the electron can also be accelerated in the direction $(-e)v_y \times B_z = A_x$ (x direction), in addition to A_y via the process of the $V_p \times B$ acceleration. The A_x component is *almost* along the magnetic field lines, as long as θ is close to $\pi/2$. As a result, the electron is accelerated three dimensionally, and the maximum velocity v_x^m in the x direction could become $2V_E$, where $V_E = cE/B_0$ is the maximum velocity of an electron accelerated in the y direction at $\theta = \pi/2$. This process has originally been predicted by Sugihara *et al.*⁶

The experiments are performed with a cylindrical, nonuniform plasma produced in a chamber of 1-m length by 60-cm diameter covered with multidipole magnets as schematically shown in Fig. 1. The precise explanations of the experimental apparatus were given elsewhere.⁵ Here, the typical parameters are given as follows: Maximum plasma density is about $2 \times 10^{11} \text{ cm}^{-3}$, electron

temperature $T_e \approx 2.0\text{--}3.0 \text{ eV}$, ion temperature $T_i \approx T_e / (10\text{--}12)$, in a neutral argon pressure of $(4\text{--}5) \times 10^{-4}$ Torr under a base pressure 2×10^{-6} Torr. As the plasma source is located at one end of the chamber, there exists a density gradient along the chamber axis (z direction) with typical gradient scale length $L = (\partial \ln n / \partial z)^{-1} \approx 100\text{--}150 \text{ cm}$ and also along the radial direction $L_r = (\partial \ln n / \partial r)^{-1} \approx 50 \text{ cm}$.

A weak magnetic field, less than 11 G, produced by two coils outside of the chamber is applied vertically (x

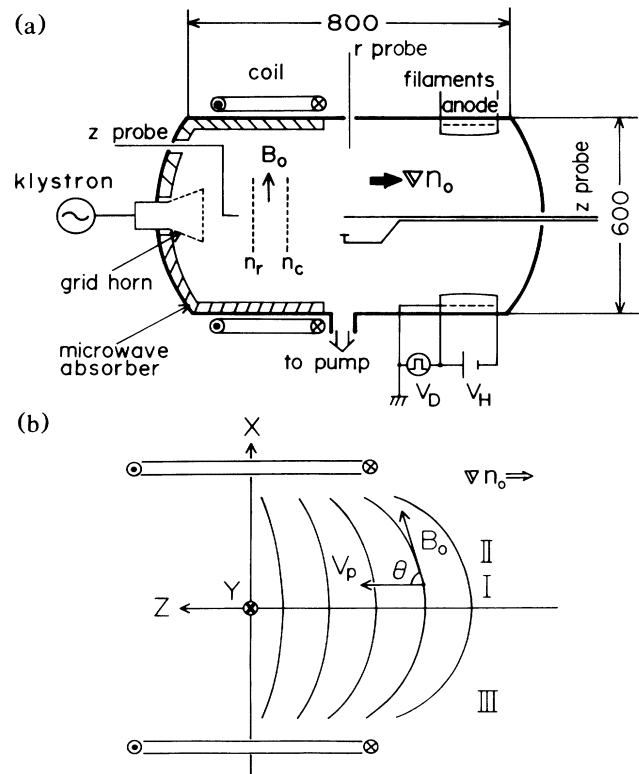


FIG. 1. Schematic structure of the experimental apparatus. (a) Whole system of the experimental apparatus, and (b) the schematic description of the oblique propagation of ES wave with angle θ to the magnetic-field lines.

direction) including regions of the present experiments. The magnetic field is made a weak mirror, the center of which is located at $z \approx 28$ cm measured from the edge of the horn antenna for the microwave irradiation [see Fig. 1(b)].

The p -polarized electromagnetic wave (EM wave) with frequency $f = (\omega/2\pi) = 2.86$ GHz and maximum power 11 kW is launched along the chamber axis from a high-gain horn antenna located at the lower-density end of the chamber. The EM wave is reflected back at the reflection layer with electron density $n_r = n_c \cos^2 \alpha$, and it excites the electron plasma wave (ES wave) around the critical layer $n_c \approx m\omega^2/4\pi e^2 \approx 1 \times 10^{11} \text{ cm}^{-3}$, where the angle of incidence α is $6^\circ - 9^\circ$ in the present experimental conditions. The ES wave with (ω, k) propagates down the density gradient, and its wave front is almost parallel to the equidensity line. When we shift up the critical layer along the z axis, the propagation direction θ between k and B can be changed through $20^\circ \leq \theta \leq 90^\circ$ (in the $x \neq 0$ area), because of the bending of the magnetic field lines [see Fig. 1(b)], while the magnetic field strength does not change in the y direction within our experimental area.

Most of the data are measured by several kinds of probes including a cylindrical probe of 0.5-mm diameter by 1-mm length for rf field measurements, and one-sided square probes of $1 \times 1 \text{ mm}^2$ for analyzing electron energy. All of these probes are movable along the z direction and rotatable around the off-center z axis for measuring the electron current shot out in the x and/or y direction. All the data are analyzed on the oscilloscope screen or on the x - y recorder chart after use of the boxcar integrator with a typical gate width of 50 nsec.

An example of accelerated high-energy electron flux with energy over 60 eV shot out in the x direction, I_{hx} , is shown in Fig. 2(a), in which we have observed, typically, two peaks on the z axis, one at the critical layer (denoted as Z_c), and the other in the lower-density area (Z_h). Here, we focused our attention on the high-energy electrons produced in the lower-density area, Z_h . Strong high-energy electron emissions are also observed if we look at the y component exactly in the y - z plane (at $x=0$). This is consistent with the results of the pure $V_p \times B$ acceleration observed previously.^{4,5}

When we shift the critical layer deeper into the chamber, that is, further away from the horn-antenna edge, by changing the plasma density slightly, the amplitude of I_{hx} at Z_h becomes first larger and then smaller again after passing through the maximum value as seen in Fig. 2(a). The shifting-up of the critical layer corresponds to making the propagation angle θ smaller.

The maximum amplitude of I_{hx} (denoted as I_{hx}^m) observed at each $z = Z_h$ is depicted as a function of Z_h in Fig. 2(b). In this figure, we clearly see that there is no major peak of high-energy electron production in the region $Z_h \geq 38$ cm without a magnetic field. When the magnetic field is applied, however, strong high-energy

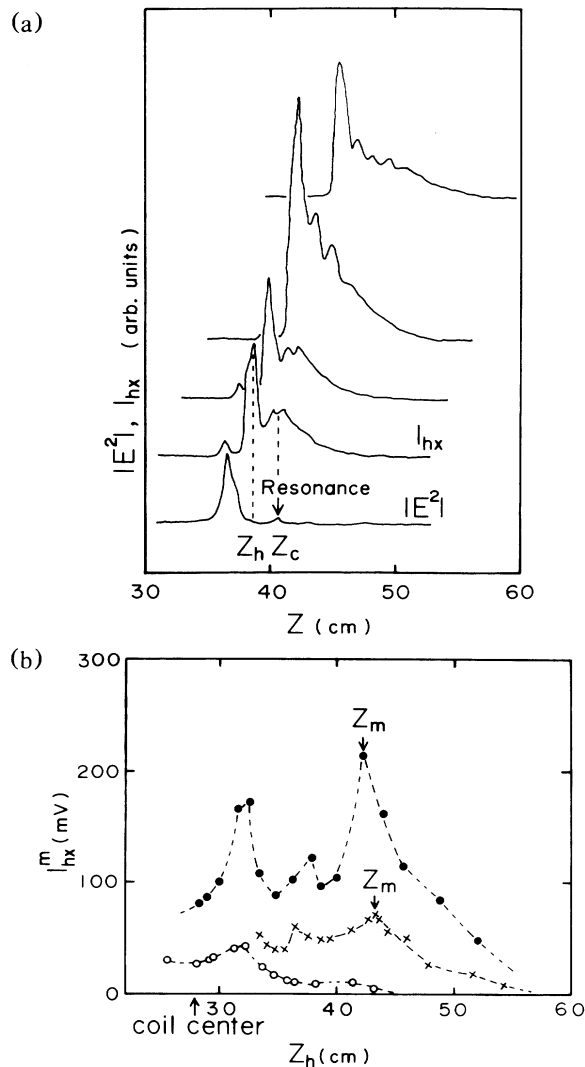


FIG. 2. (a) High-energy electron flux, I_{hx} , with energy ≥ 60 eV produced in the x direction vs the z axis with the change of the plasma density as a parameter. $P = 4.8$ kW and $B_0 = -5$ G. (b) The maximum value of I_{hx} , I_{hx}^m , observed at each $z = Z_h$ as a function of Z_h depicted from (a). Open circles stand for $B_0 = 0$ and $P = 2.3$ kW; otherwise $B_0 = -5$ G with rf power 1.0 kW for crosses, and 4.8 kW for filled circles.

electron production is observed which depends on the microwave irradiation power. Here, we should mention that the position where I_{hx}^m has the maximum value at $Z_h = Z_m$ also changes with rf power [see Fig. 2(b)].

The high-energy electrons in the x direction have dependence on propagation angle θ as shown in Fig. 3. Here, the experimental data are depicted from Fig. 2(b) for $P = 1.0$ kW with the assumption that the high-energy electron flux I_{hx}^m is in proportion to v_x , and θ is converted from Z_h by the use of the calculated spatial profile of the magnetic field, such as schematically shown in Fig. 1(b). From this figure, we can obtain the optimum angle θ_c

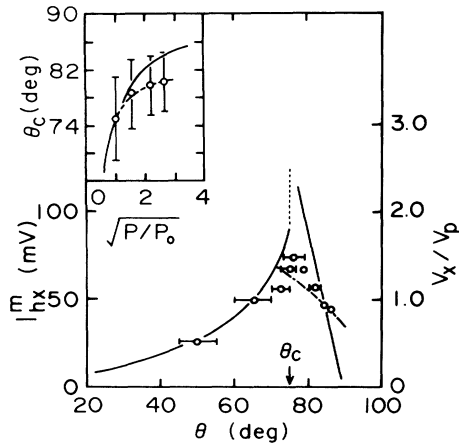


FIG. 3. High-energy electron flux, I_{hx}^m (open circles), and calculated value of v_x (solid and dash-dotted line), vs the propagation angle θ . The experimental data are depicted from Fig. 2(b) for $P=1.0$ kW. Inset shows the optimum angle θ_c vs the square root of rf power normalized by $P_0=1$ kW at $B_0=-5$ G. Solid line in the inset shows the results of Eq. (1).

which corresponds to Z_m . Therefore, it is possible to depict the dependence of θ_c on the rf power as shown in the inset of Fig. 3. The error bars in the figure come mainly from the fact that the ES wave travels to accelerate electrons for a certain distance along which the angle θ changes continuously.

An example of I_{hx}^m vs the rf power is shown in Fig. 4. In this figure, we also show the high-energy electron flux I_{hx} shot out in the x direction observed at $z=Z_c$ (critical layer). The electron flux, I_{hx} , increases linearly with the increase of rf power up to 1.5 kW, while I_{hx}^m has the threshold value at $P \approx 200$ W, because the ES wave field should have finite value for trapping electrons into a wave field.⁵ This is consistent with the phenomena observed in the $V_p \times B$ acceleration at $\theta = \pi/2$.

In order to interpret the experimental results, we have used the theory based on the model of initially deeply trapped electrons.⁶ By use of Eqs. (5) and (8) in Ref. 6, numerical results for $\theta_c = 74^\circ$ are obtained as shown by a solid line in Fig. 3. In the present experiment, the maximum acceleration length in the x direction is restricted to less than about 4–5 cm because of the detector systems. Therefore, we could use the acceleration time $\approx 1/\omega_{cz}$ in calculating the theoretical value v_x , where $\omega_{cz} = \Omega \cos\theta$, and Ω is the electron cyclotron frequency. The acceleration length would exceed the present system when $65^\circ - 70^\circ \leq \theta \leq 90^\circ$ in Fig. 3, while for $\theta \leq 60^\circ$, a maximum value of v_x can be expected within this acceleration time. In calculating the velocity v_x in the range $70^\circ \leq \theta \leq 90^\circ$, we may use the constant acceleration length $x \approx 5$ cm, and the result is shown in the same figure by a dash-dotted line, showing reasonable agreement with the theoretical result. The same result has also been obtained in the higher-power case not

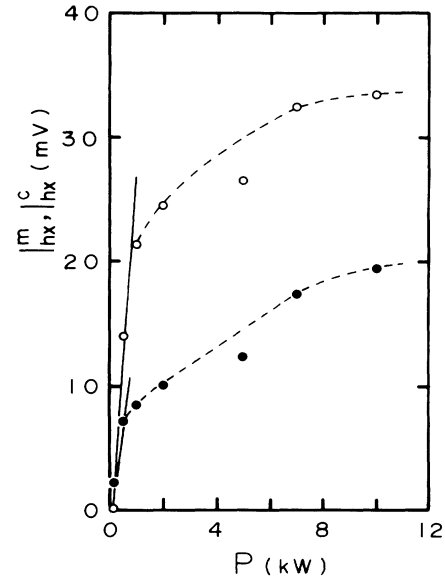


FIG. 4. Dependence of high-energy electron flux on the input rf power. Open circles stand for I_{hx}^m and filled circles for I_{hx} . $B_0 = -5$ G.

shown here, although the coincidence is weaker in this case because of the effect of saturation (see Fig. 4).

The optimum angle θ_c is also calculated as a function of electric field strength. The angle θ_c is given as follows⁶:

$$\sin\theta_c = \{2/[1 + (1 + 4V_p^2/V_E^2)^{1/2}]\}^{1/2}. \quad (1)$$

The result is shown in the inset of Fig. 3 by a solid line obtained with our parameters. Here, both of the results of experiments and theory are adjusted at $(P/P_0)^{1/2} = 1.0$ after assuming that the electric field strength of the ES wave is in proportion to the square root of the incident power of the EM wave. When we take the experimental results of $V_p \approx (3-5) \times 10^8$ cm/sec and $V_E \approx 1.0 \times 10^9$ cm/sec, $\theta_c \approx 74^\circ - 66^\circ$ is obtained, which can be compared with the experimental results of $\theta_c \approx 74^\circ$ seen in Fig. 3. This difference comes from the ambiguity for determining the phase velocity and the absolute value of the electric field strength of the ES wave. The above-mentioned parameters V_E and V_p are obtained separately, but in the same experimental conditions, from the method of high-energy electron production observed in the y direction through the process of $V_p \times B$ acceleration with $\theta = \pi/2$.^{4,5} For determining the angle θ , we used the calculated value of the magnetic field profile in space. Therefore, there may be some ambiguities in angle, probably several degrees.

In the theory, the maximum velocity of electrons in the x direction, v_x^m , could be $2V_E$, and the acceleration time responsible for this acceleration is $\tau_a = \pi t_a$, where $t_a = V_E/\Omega V_p$ is the acceleration time with $\theta = \pi/2$. With

the present parameters, typically, $t_a \approx 42$ nsec and so $\tau_a \approx 130$ nsec are obtained, and the maximum acceleration length, l , corresponding to τ_a in the x direction at $\theta = 74^\circ$ is about $l \approx 40$ cm over our plasma size. Thus, the electrons cannot be accelerated up to the maximum velocity for $\theta > 70^\circ$ in the present machine. Therefore, the relation $v_x^m \approx 2V_E$ was not confirmed. Most of the observed characteristics, however, are well interpreted by the theoretical prediction of Sugihara *et al.*⁶

In conclusion, we have observed, for the first time, high-energy electrons accelerated *almost* along the magnetic-field lines in microwave-plasma interaction experiments. This process can be interpreted consistently by the $V_p \times B$ acceleration mechanism, in which the driving electrostatic wave propagates *obliquely* to the magnetic field B .

The authors are indebted to Dr. R. Sugihara for his valuable discussions and comments. Thanks are given to Dr. N. Asano for his comments and proofreading. A part of the present work is supported by a Grant-in-Aid

for Scientific Research from the Ministry of Education, Science and Culture, Japan.

¹R. Z. Sagdeev and V. P. Shapiro, Pis'ma Zh. Eksp. Teor. Fiz. **17**, 389 (1973) [JETP Lett. **17**, 279 (1973)].

²R. Sugihara and Y. Midzuno, J. Phys. Soc. Jpn. **47**, 1290 (1979).

³J. M. Dawson, V. K. Decyk, R. W. Huff, I. Jechart, T. Katsouleas, J. N. Leboeuf, and M. Martinez, Phys. Rev. Lett. **50**, 1455 (1983).

⁴Y. Nishida, M. Yoshizumi, and R. Sugihara, in Proceedings of the Thirteenth Annual Anomalous Absorption Conference, Banff, Alberta, Canada, 1983 (unpublished), p. F7, and Phys. Lett. **105A**, 300 (1984), and Phys. Fluids **28**, 1574 (1985).

⁵Y. Nishida, N. Y. Sato, and T. Nagasawa, IEEE Trans. Plasma Sci. **15**, 243 (1987).

⁶R. Sugihara, S. Takeuchi, K. Sakai, and M. Matsumoto, Phys. Rev. Lett. **52**, 1500 (1984).